# Effects of Annealing and Prior History on Enthalpy Relaxation in Glassy Polymers. 4. Comparison of Five Polymers

**Ian M. Hodge**

*BFGoodrich Research and Development Center, Brecksville, Ohio 44141.*
*Received October 27, 1982*

ABSTRACT: Parameters for enthalpy relaxation in and below the glass transition temperature range were determined for poly(vinyl acetate) (PVAc), poly(methyl methacrylate) (PMMA), and bisphenol A polycarbonate (PCarb) and compared with those previously obtained for another PVAc, two polystyrenes (PS), poly(vinyl chloride) (PVC), the inorganic glasses $As_2Se_3$ and $B_2O_3$, and the simple organic glass 5-phenyl 2-ether. The four-parameter treatment of Moynihan and co-workers was found to give an adequate description of the relaxation component of the heat capacity, as a function of cooling rate, annealing temperature, and annealing time, for PVAc and PCarb. Significant deviations were found for PMMA. Strong correlations were observed between all four parameters for the five polymers, which were interpreted in terms of a cooperative relaxation mechanism.

## Introduction

Annealing of amorphous polymers below the glass transition temperature range produces changes in many physical properties such as density, complex permittivity, enthalpy, complex mechanical modulus, and creep compliance. A particularly convenient property for the study of annealing is enthalpy, because of the availability of accurate and sensitive DSC instruments. The decrease in enthalpy during annealing is recovered during reheating to above the glass transition, and this recovery is usually manifested as a maximum in the heat capacity at temperatures ranging from well below to near the upper edge of the glass transition range. Recovery of the enthalpy lost during annealing has been observed in many polymeric materials,[1-18] and a sufficiently large amount of experimental data has now been collected to permit several generalizations to be made:

(1) The temperatures, $T_{max}$, at which the heat capacity maxima, $C_{p_{max}}$, occur increase approximately linearly with annealing temperature, $T_e$, and the log of the annealing time, $t_e$, provided the aged glass is not too close to equilibrium. Also, $T_{max}$ increases approximately linearly with the log of the heating rate, $Q_H$. It also appears that $T_{max}$ is insensitive to the history before aging, such as cooling rate,[18] vapor-induced swelling,[18] hydrostatic pressure applied during cooling,[5,9,11,15] or mechanical straining.[6,16,18]

(2) The magnitude of $C_{p_{max}}$ also increases approximately linearly with $T_e$ and log $t_e$, again providing that the aged glass is not too close to equilibrium. In contrast to $T_{max}$, however, $C_{p_{max}}$ is a strong function of prior history. Generally speaking, those histories that elevate the enthalpy of the glass before annealing serve to increase $C_{p_{max}}$. Similar behavior is observed for the enthalpy lost during aging, $\Delta H$, of which $C_{p_{max}}$ is a crude measure.

(3) As the aged glass approaches equilibrium deviations from these linear relations are observed, until at equilibrium no changes occur with annealing. At fixed $t_e$, $\Delta H$ and $C_{p_{max}}$ pass through maxima as a function of $T_e$, often when $T_e$ is about 20 K below the center of the glass transition range, $T_g$, and decreases to zero when $T_e$ is well above $T_g$. At fixed $T_e$, $\Delta H$ becomes constant at long $t_e$ as the aged glass approaches equilibrium.

The first reported observations of heat capacity maxima well below $T_g$ in aged glasses appear to be those of Illers.[1] The first theoretical account of this phenomenon was that of Kovacs et al.,[19] given in terms of a multiparameter model for the glass transition which included the well-established nonlinearity and nonexponentiality (relaxation time distribution) of the glass transition kinetics. Recently Hodge and Berens[20] gave a physically similar, but mathematically different, account in terms of the four-parameter treatment of the glass transition kinetics by Moynihan and co-workers[21] and demonstrated explicitly that all of the general features listed above could be reproduced by this approach. Good fits to data for poly(vinyl chloride) (PVC) were also obtained for several combinations of $T_e$ and $t_e$. Hodge and Huvard[22] demonstrated that the four parameters of the Moynihan formulation could be optimized by using a standard computer search routine, and applied this optimization procedure to data for two polystyrenes (PS). For the present work essentially the same technique was applied to data for poly(vinyl acetate) (PVAc), poly(methyl methacrylate) (PMMA), and bisphenol A polycarbonate (PCarb). The enthalpy relaxation parameters for these materials were compared with those already found for PVC,[20] PS,[22] another PVAc,[23] $B_2O_3$,[21] $As_2Se_3$,[24] and the lubricating oil $C_6H_5(OC_6H_4)_3OC_6H_5$ ("5-phenyl 4-ether" or "5P4E")[24] by using the same formalism.

For convenience we outline the treatment of the glass transition kinetics of Moynihan and co-workers,[21] how annealing was introduced by Hodge and Berens,[20] and the optimization procedure used by Hodge and Huvard.[22] The glass transition kinetics are characterized by two essential features—nonexponentiality (relaxation time distribution) and nonlinearity. The Moynihan approach linearizes the kinetics by using the method of Gardon and Narayanaswamy,[25,26] considers cooling and heating as a series of temperature steps, and applies Boltzmann superposition of nonexponential responses to the temperature steps. As a matter of convenience, and good accuracy, the response function is chosen to be of the Williams–Watts[27,28] form

$$\phi(t) = \exp[-(t/\tau_o)^\beta] \quad (1)$$

where $1 \geq \beta > 0$ and $\tau_o$ is a relaxation time which depends on temperature, $T$, and fictive temperature,[29] $T_f$, as

$$\tau_o = A \exp\left(\frac{x\Delta h^*}{RT} + \frac{(1-x)\Delta h^*}{RT_f}\right) \quad (2)$$

where $A$, $x$ ($1 \geq x > 0$), and $\Delta h^*$ are parameters and $R$ is the ideal gas constant. The four parameters $\beta$, $A$, $x$, and $\Delta h^*$ are assumed to be independent of $T$ and $T_f$. Hodge and Berens[20] introduced annealing into the cooling cycle, with the annealing time divided into ten logarithmically even spaced subintervals to allow for nonlinearity during annealing. Hodge and Huvard[22] used an optimization technique based on the Marquardt search routine.[30] The thermal history (cooling rate, annealing temperature, annealing time, and reheating rate) and $\Delta h^*$ were input, and the best fit values of $A$, $x$, and $\beta$ were output. The best-fit

Table I
Polymer Molecular Weights

| material | $M_{\text{w}}$ | $M_{\text{n}}$ | $M_{\text{w}}/M_{\text{n}}$ | ref |
|---|---|---|---|---|
| PVAc | $1.95 \times 10^5$ | $4.77 \times 10^4$ | 4.1 | this work |
| PVAc | $2.0 \times 10^6$ | $3.4 \times 10^5$ | 5.9 | 23 |
| PVC | $2.05 \times 10^5$ | $6.5 \times 10^4$ | 3.2 | 18 |
| PS | $3.21 \times 10^5$ | $8.46 \times 10^4$ | 3.8 | 22 |
| PS | $2 \times 10^5$ | $2 \times 10^5$ | <1.06 | 17 |
| PMMA | $6.06 \times 10^4$ | $3.32 \times 10^4$ | 1.8 | this work |
| PCarb | $3.38 \times 10^4$ | $1.34 \times 10^4$ | 2.5 | this work |

value of $\Delta h^*$ was obtained from the minimum in residual sum of squares deviation as a function of $\Delta h^*$. For the present work, $\Delta h^*$ was determined from the cooling rate dependence of the frozen in fictive temperature $T_f'$:[21]

$$\frac{\text{d} \ln Q_{\text{C}}}{\text{d}(1/T_f')} = -\Delta h^*/R \qquad (3)$$

## Experimental Section

All three materials were Aldrich Secondary Standards. Weight-average and number-average molecular weights are given in Table I, together with those of other materials for which the enthalpy relaxation parameters are known. The materials studied here were dried for 2 h or more at about 30 °C above $T_g$ before being sealed into the DSC pans. Sample weights were about 10 mg. Each sample was left untouched in the DSC instrument between runs to reduce experimental scatter due to changes in thermal transfer between the instrument cell and sample pan. Three repeat scans were performed during the course of the annealing experiments to test for possible thermal decomposition and estimate experimental uncertainty. For these repeat scans cooling at 40 K min$^{-1}$ from well above $T_g$ to well below $T_g$ was followed by immediate reheating at 10 K min$^{-1}$, with no intervening annealing. For convenience, we shall refer to this thermal history as $-40/+10$, with appropriate changes for other cooling rates. The upper and lower temperature limits for all thermal histories were 220 and 350 K for PVAc, 300 and 450 K for PMMA, and 350 and 510 K for PCarb. The heating rate was fixed at 10 K min$^{-1}$. All measurements were made with a Perkin-Elmer DSC-2.

Experimental data $C_p(T)$ were normalized with respect to the difference between liquid and glassy heat capacities, $C_{p_l}$ and $C_{p_g}$, respectively:

$$C_p^N = \frac{C_p(T) - C_{p_g}(T)}{C_{p_l}(T) - C_{p_g}(T)} \qquad (4)$$

These normalized data are directly comparable with the calculated values. The temperature dependences of $C_{p_l}$ and $C_{p_g}$ were obtained by linear extrapolation of the liquid- and glassy-state data. The temperature dependence of $C_{p_l}$ was always linear, and extrapolation into the transition range was not subject to significant uncertainty. When $C_{p_g}$ was extrapolated, care was taken to ensure that only the lowest temperature range data were used (more than $\sim$40 K below $T_g$), since relaxation effects associated with aging and the glass transition can make a significant contribution to $C_p$ well below the transition range, according to calculations.

Three sets of experiments were performed. In the first, the cooling rate was varied (40, 20, 10, and 5 K min$^{-1}$) with no annealing. In the second, the annealing time was fixed at 1 h at
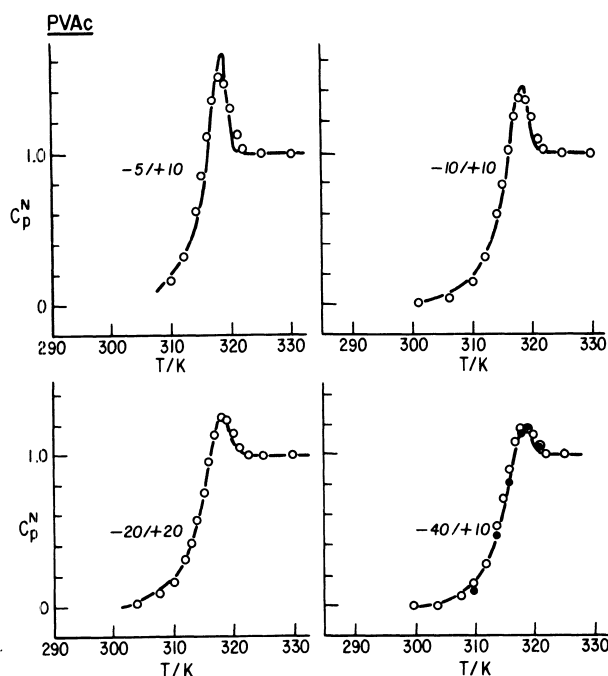


**Figure 1.** Experimental points and fits for $C_p^N$ as a function of cooling rate for PVAc. Best fit parameters given in Table II.

annealing temperatures which were ca. 30, 20, and 10 K below $T_g$ (for present purposes $T_g$ is defined as the temperature at which $C_p^N = 0.5$, measured at 10 K min$^{-1}$ after cooling at 40 K min$^{-1}$). In the third set of experiments, the annealing temperature was fixed at ca. 30 K below $T_g$ for annealing times of 1 and $\sim$16 h. The cooling rate was fixed at 40 K min$^{-1}$ for all annealing experiments, and annealing was performed in the cooling cycle.

The optimization procedure for obtaining best-fit parameters is outlined above and described in detail elsewhere.[22] Best-fit parameters were obtained for each thermal history and averaged. The averages were heavily weighted by the thermal histories that were most difficult to fit. These were for PVAc $t_e = 1$ h, $T_e = 300$ K; for PMMA $t_e = 17$ h, $T_e = 350$ K; for PCarb $t_e = 16$ h, $T_e = 390$ K.

## Results

The random experimental scatter in $C_{p_{max}}^N$ (the maximum in $C_p^N$ just above $T_g$) for the repeated $-40/+10$ scans was $\pm 5\%$. No systematic changes of more than ca. 5% were observed, indicating no significant decomposition. For PVAc and PCarb the estimated uncertainties in the best fit parameters were $\pm 0.05$ in $x$ and $\beta$, $\pm 10\%$ in $\Delta h^*$, and $\pm 1.0$ for $\ln A$. For PMMA the best fits were poorer and the uncertainties were twice as large (see Discussion). The fits to experimental data for PVAc are shown in Figures 1 and 2, for PMMA in Figures 3 and 4, and for PCarb in Figures 5 and 6. Only two 1-h annealing experiments were performed for PVAc. Sets of best-fit parameters for these three materials, together with those obtained previously for the other polymers listed in Table I, two inorganic glasses and a lubricating oil, are given in

Table II
Enthalpy Relaxation Parameters

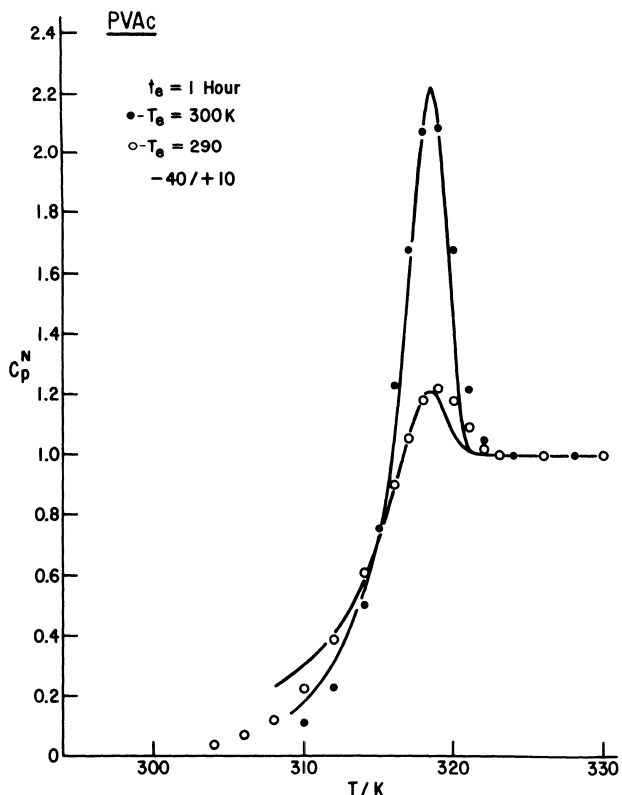| material | $\ln A$ (s) $\pm$ 1 | $\Delta h^*/10^3 R \pm 10\%$, K | $x \pm 0.05$ | $\beta \pm 0.05$ | ref |
|---|---|---|---|---|---|
| PVAc | $-275.4$ | 88 | 0.28 | 0.53 | this work |
| PVAc | $-223.6$ | 71.3 | 0.41 | 0.51 | 23 |
| PVC | $-619.0$ | 225 | 0.11 | 0.25 | 18 |
| PS | $-216.4$ | 80 | 0.43 | 0.68 | 22 |
| PS | $-457.0$ | 175 | 0.12 | 0.39 | 17 |
| PMMA | $-355.7$ | 138 ($\pm 20\%$) | 0.22 ($\pm 0.1$) | 0.37 ($\pm 0.1$) | this work |
| PCarb | $-353.6$ | 150 | 0.22 | 0.54 | this work |
| $As_2Se_3$ | $-85.5$ | 40.9 | 0.49 | 0.67 | 24 |
| $B_2O_3$ | $-75.6$ | 45 | 0.40 | 0.65 | 21 |
| 5P4E | $-153.1$ | 38.5 | 0.40 | 0.70 | 24 |

**Figure 2.** Experimental points and fits for $C_p^N$ for the indicated combinations of $T_e$ and $t_e$ for PVAc. Parameters same as in Figure 1.
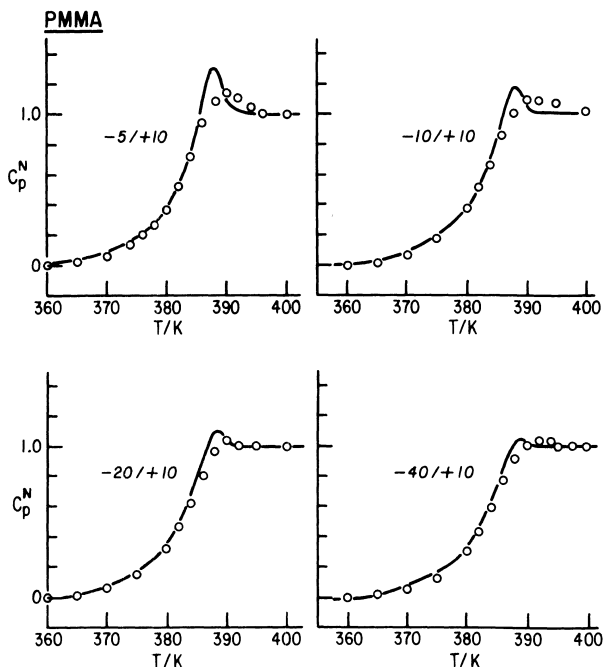


**Figure 3.** Experimental points and fits for $C_p^N$ as a function of cooling rate for PMMA. Best fit parameters given in Table II.



**Figure 4.** Experimental points and fits for $C_p^N$ for the indicated combinations of $T_e$ and $t_e$ for PMMA. Parameters same as in Figure 3.



**Figure 5.** Experimental points and fits for $C_p^N$ as a function of cooling rate for PCarb. Best fit parameters given in Table II.

Table II. These parameters were all obtained by using the Moynihan formulation, and are thus directly comparable.

## Discussion

The fits for PVAc (Figures 1 and 2) and PCarb (Figures 5 and 6) deviate from the data by less than the experimental uncertainty, indicating that the model provides an adequate account of enthalpy relaxation in these materials. The fits to PMMA deviate from the experimental data by
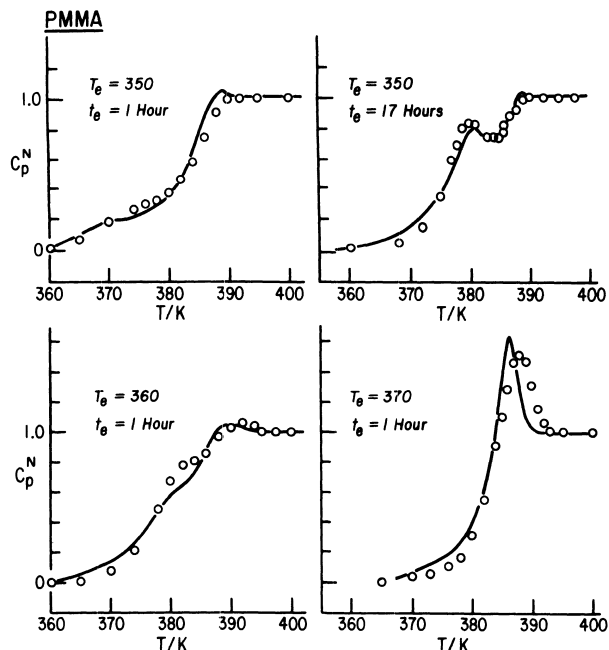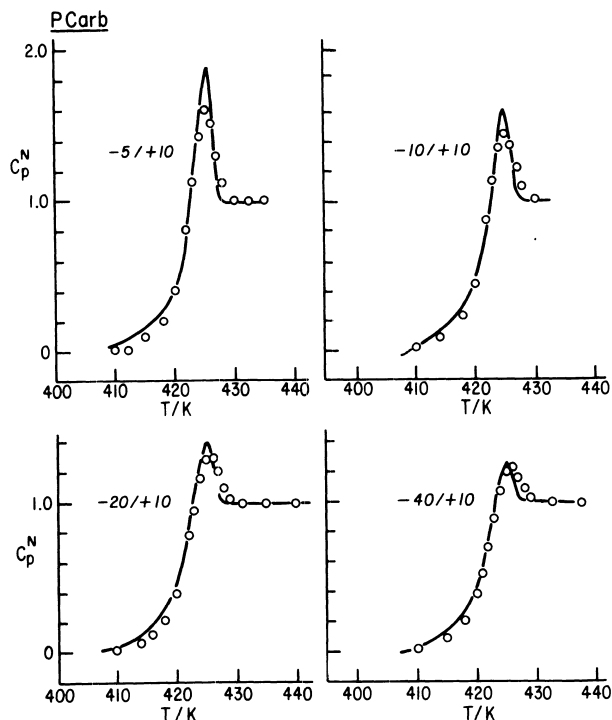
up to 17%, well outside experimental uncertainty, although the occurrence of sub-$T_g$ shoulders and maxima in $C_p^N$ in annealed glasses is qualitatively reproduced. Evidently there is at least one feature of the enthalpy relaxation kinetics for PMMA that is not being properly accounted for in the model. Accordingly, the uncertainties in the enthalpy relaxation parameters for PMMA are larger than those for the other materials (see Table II).

The parameters obtained for PVAc agree within uncertainty limits with those obtained by Sasabe and Moynihan,[23] except for $x$, where the difference is slightly greater than the sum of uncertainties. The similarity of the enthalpy relaxation parameters for these two PVAc materials
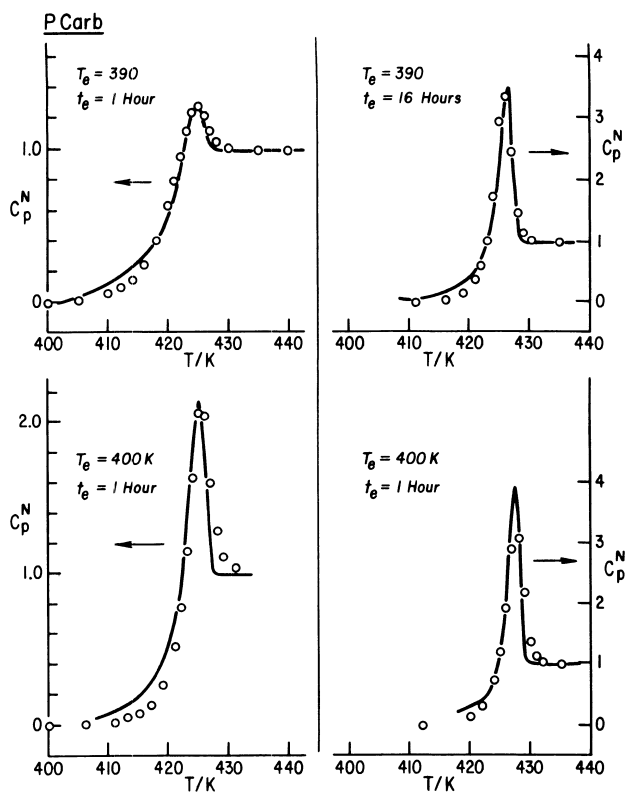
**Figure 6.** Experimental points and fits for $C_p^N$ for the indicated combinations of $T_e$ and $t_e$ for PCarb. Same parameters as in Figure 5.
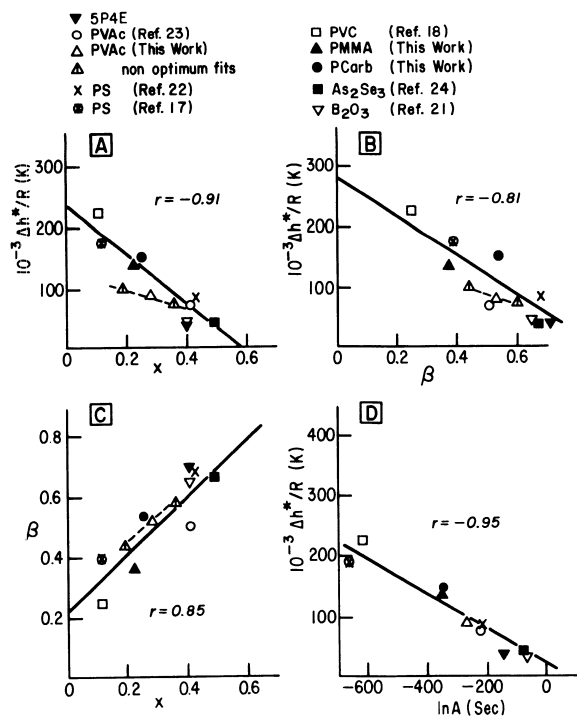


**Figure 7.** Correlations between pairs of enthalpy relaxation parameters for the materials listed in Table II. The axes are (A) $\Delta h^*/R$ and $x$, (B) $\Delta h^*/R$ and $\beta$, (C) $\beta$ and $x$, and (D) $\Delta h^*/R$ and $\ln A$. Lines are least-squares best fits. Correlation coefficients are denoted by $r$. The sets of three points for PVAc (present work) illustrate correlations of parameter uncertainties (see text).

is in sharp contrast with the large differences in parameters for two PS materials studied earlier[22] (see Table II). It should be noted, however, that the parameters for one of these polystyrenes (obtained from data published by Chen and Wang[17]) are somewhat uncertain because they were obtained for only two thermal histories, and no directly determined experimental value of $\Delta h^*$ was available. It is therefore possible that the parameters for this PS are not optimum for all thermal histories and that the differences between the two polystyrenes are not as large as the parameters in Table II indicate.

An inspection of the data shown in Table II reveals a strong correlation between the parameters $\beta$, $x$, $\Delta h^*$, and $\ln A$. The correlations between $\Delta h^*$ and $x$, $\Delta h^*$ and $\beta$, $x$ and $\beta$, and $\ln A$ and $\Delta h^*$ are displayed in Figure 7. The corresponding linear correlation coefficients are −0.93, −0.91, +0.85, and −0.95, respectively. The correlations are robust with respect to uncertainties in the parameters: varying $\Delta h^*$ in the optimization program produces tetrads of $\Delta h^*$, $x$, $\beta$, and $\ln A$ that move along all four correlation lines. To illustrate this pairs of parameters for the averaged −40/+10 scans for PVAc, in which $\Delta h^*/R$ was varied by ca. ±15% from its experimental value, are shown in each of the correlation plots. The observed correlations do not appear to be artifacts of the uncertainties, however, since the uncertainties are small compared with the total variation (with the possible exception of the PS material discussed above). We shall therefore accept the correlations as established for the materials considered here and proceed to discuss their implications.

The correlation between $\Delta h^*$ and $A$ results from the relatively small range in $T_g$ for the materials considered here. The value of $\tau_0$ (eq 2) is approximately 100 s at $T_g$, and since $T_f \sim T$ at $T_g$ eq 2 yields

$$\ln A = \ln (100) - (\Delta h^*/RT_g) \tag{5}$$

Thus $-\ln A$ is directly proportional to $\Delta h^*$ for similar

values of $T_g$. Correspondingly, when $\Delta h^*$ is fixed (e.g., by eq 3) $\ln A$ essentially determines $T_g$ ($x$ and $\beta$ have a relatively minor effect on $T_g$).

In discussing the other correlations we first observe that the enthalpy relaxation model used here is phenomenological and that any molecular interpretation of its parameters is made at some risk. With this in mind, we now suggest tentative molecular interpretations of $\beta$, $\Delta h^*$, and $x$ whose chief merit is to make the correlations between these parameters self-consistent.

The parameter $\beta$ may be regarded as reflecting the breadth of distribution of relaxation times or as a direct measure of the departure from an exponential decay function (single relaxation time). Although these two interpretations are mathematically equivalent, they reflect different physical emphases. When a relaxation is described in terms of a relaxation time distribution it is not unusual to identify individual relaxation time components with physically distinct processes. For example, a change in shape of the distribution with temperature is sometimes regarded as reflecting different activation enthalpies for the processes corresponding to the different relaxation time components. When viewed as a measure of nonexponentiality, $\beta$ can be interpreted as a measure of degree of cooperativity of the relaxation process. In this case, changes in $\beta$ with temperature correspond to changes in the degree of cooperativity. Here we interpret $\beta$ as a measure of cooperativity, which can be usefully defined in terms of the number of chain segments involved in a particular relaxation event. Low values of $\beta$ correspond to a high degree of cooperativity and a large number of chain segments. If it is assumed that the activation enthalpy per segment is a weak function of polymer type, the involvement of a large number of chain segments would result in a large activation enthalpy for the relaxation event ($\Delta h^*$). The observed inverse correlation between $\beta$ and $\Delta h^*$ (Figure 7B) is consistent with this, suggesting that the

activation energy per segment is indeed a weak function of polymer type. Some support for this reasoning is found in the theory recently proposed by Bendler and Ngai[31] for volume recovery in amorphous polymers. This theory provides theoretical support for the Williams–Watts response function, with $\beta$ determined by the number of correlated low energy states in the heat bath around a reference molecule and by the strength of coupling between the heat bath and conformational states of the molecule. A result of this theory is that the apparent activation energy, corresponding to $\Delta h^*$, is given by $E_A/\beta$, where $E_A$ is the barrier height between conformations of adjacent segments. In terms of this theory, the observed inverse correlation between $\beta$ and $\Delta h^*$ suggests that $\Delta h^*$ is determined more by the strength of coupling between conformational states and the heat bath (i.e., degree of cooperativity) than by the intramolecular energy barrier between conformational states. We also observe that the clustering of parameters for $B_2O_3$, $As_2Se_3$, and 5P4E around the maximum observed values of $x$ and $\beta$ and minimum value of $\Delta h^*$ (Table II) supports the idea that enthalpy relaxation in these materials is less cooperative than in polymers.

The parameter $x$ is a measure of the relative importance of macroscopic structure (as defined by $T_f$) and temperature in determining the average relaxation time, and it is natural to extend this to the molecular level by interpreting "structure" in molecular terms such as chain conformations and their correlations. A more cooperative relaxation mechanism involving many chain segments would be expected to be more strongly influenced by molecular structure (smaller $x$), in agreement with the observed correlations $x$, $\beta$, and $\Delta h^*$. Also, the inverse correlation between $x$ and $\Delta h^*$ results in the product $x\Delta h^*$ being a weak function of polymer type. (For the polymers considered here the standard deviation for $x\Delta h^*$ is 5% of the mean, compared with 40% for $\Delta h^*$.) Thus the activation enthalpy for chain diffusion above $T_g$ ($\Delta h^*$) is a stronger function of polymer type than the activation enthalpy for molecular motion in the glassy state ($x\Delta h^*$). The glassy state behavior is consistent with relatively localized motions dominating the temperature dependence of relaxation processes in the glassy state and with the suggestion offered above that the activation enthalpy per chain segment does not depend strongly on polymer type. On the other hand, the isothermal structural dependence of the average relaxation time in the glassy state, which determines the rate of physical aging and of which $(1-x)\Delta h^*$ is a direct measure, is an even stronger function of polymer type than the temperature dependence above $T_g$ (the standard deviation for $(1-x)\Delta h^*$ is 72% of the mean). This is consistent with the expectation that highly cooperative motions involving a large number of chain segments (low $\beta$, high $\Delta h^*$) are strongly affected by polymer type and molecular structure in the glassy state.

## Summary and Conclusions

The correlations shown in Figure 7 appear to be real and not artifacts of correlated uncertainties in the parameters, although the latter possibility cannot be completely ruled out. The correlations are all consistent with the well-es-tablished cooperativity of the glass transition kinetics. To the extent that the five polymers considered here are representative of polymers in general, it also appears that the phenomenological enthalpy relaxation parameters $\beta$, $\Delta h^*$, and $x$ reflect cooperative molecular relaxation processes, although their relationship to specific molecular details of different polymers is obscure at this time. Characterizations of enthalpy relaxation in more polymers are needed to establish how general the correlations are and to what extent the enthalpy relaxation parameters can be identified with specific molecular features.

**Registry No.** PVAc, 9003-20-7; PMMA, 9011-14-7; PCarb, 24936-68-3; carbonic acid–bisphenol A copolymer, 25037-45-0.

## References and Notes

(1) Illers, K. H. *Makromol. Chem.* **1969**, *127*, 1.
(2) Foltz, C. R.; McKinney, P. V. *J. Appl. Sci.* **1969**, *13*, 2235.
(3) Ali, M. S.; Sheldon, R. P. *J. Appl. Sci.* **1970**, *14*, 2619.
(4) Petrie, S. E. B. *J. Polym. Sci., Polym. Phys. Ed.* **1972**, *10*, 1255.
(5) Weitz, A.; Wunderlich, B. *J. Polym. Sci., Polym. Phys. Ed.* **1974**, *12*, 2473.
(6) Brady, T. E.; Jabarin, S. A. *Polym. Eng. Sci.* **1977**, *17*, 686.
(7) Gray, A.; Gilbert, M. *Polymer* **1976**, *17*, 44.
(8) Straff, R.; Uhlmann, D. *J. Polym. Sci., Polym. Phys. Ed.* **1976**, *14*, 1087.
(9) Brown, I. G.; Wetton, R. E.; Richardson, M. J.; Savill, N. G. *Polymer* **1978**, *19*, 659.
(10) Ophir, Z. H.; Emerson, J. A.; Wilkes, G. L. *J. Appl. Phys.* **1978**, *69*, 5032.
(11) Richardson, M. J.; Savill, N. G. *Br. Polym. J.* **1979**, *11*, 123.
(12) O'Reilly, J. M. *J. Appl. Phys.* **1979**, *50*, 6083.
(13) Wysgoski, M. G. *J. Appl. Polym. Sci.* **1980**, *25*, 1455.
(14) Shultz, A. R.; Young, A. L. *Macromolecules* **1980**, *13*, 633.
(15) Prest, W. M., Jr.; O'Reilly, J. M.; Roberts, F. J., Jr.; Mosher, R. A. *Polym. Eng. Sci.* **1981**, *21*, 1181.
(16) Prest, W. M., Jr.; Roberts, F. J., Jr. *Ann. N.Y. Acad. Sci.* **1981**, *371*, 67.
(17) Chen, H. S.; Wang, T. T. *J. Appl. Phys.* **1981**, *52*, 5898.
(18) Berens, A. R.; Hodge, I. M. *Macromolecules* **1982**, *15*, 756.
(19) Kovacs, A. J.; Aklonis, J. J.; Hutchinson, J. M.; Ramos, A. P. *J. Polym. Sci., Polym. Phys. Ed.* **1979**, *17*, 1097.
(20) Hodge, I. M.; Berens, A. R. *Macromolecules* **1982**, *15*, 762.
(21) DeBolt, M. A.; Easteal, A. J.; Macedo, P. B.; Moynihan, C. T. *J. Am. Ceram. Soc.* **1976**, *59*, 16.
(22) Hodge, I. M.; Huvard, G. S. *Macromolecules* **1983**, *16*, 371.
(23) Sasabe, H.; Moynihan, C. T. *J. Polym. Sci.* **1978**, *16*, 1447.
(24) Moynihan, C. T.; Macedo, P. B.; Montrose, C. J.; Gupta, P. K.; DeBolt, M. A.; Dill, J. F.; Dom, B. E.; Drake, P. W.; Easteal, A. J.; Elterman, P. B.; Moeller, R. P.; Sasabe, H.; Wilder, J. A. *Ann. N.Y. Acad. Sci.* **1976**, *279*, 15.
(25) Gardon, R.; Narayanaswamy, O. S. *J. Am. Ceram. Soc.* **1970**, *53*, 148.
(26) Narayanaswamy, O. S. *J. Am. Ceram. Soc.* **1971**, *51*, 691.
(27) Williams, G.; Watts, D. C. *Trans. Faraday Soc.* **1970**, *66*, 80.
(28) Williams, G.; Watts, D. C.; Dev, S. B.; North, A. M. *Trans. Faraday Soc.* **1971**, *67*, 1323.
(29) Tool, A. Q. *J. Am. Ceram. Soc.* **1946**, *29*, 240.
(30) Kuester, J. L.; Mize, J. H. "Optimization Techniques with Fortran"; McGraw-Hill: New York, 1973.
(31) Bendler, J. T.; Ngai, K. L., to be published.